

phys. stat. sol. (b) **162**, 451 (1990)

Subject classification: 64.60 and 71.20; S1.4

*Institute of Physical Chemistry, Academy of Sciences of the USSR, Moscow<sup>1)</sup>*

## **Isostructural $\gamma$ - $\alpha$ Transition in Metallic Cerium as a Mott Transition**

By

G. V. IONOVA and A. V. NIKOLAEV

The isostructural  $\gamma$ - $\alpha$  phase transition of Ce is studied by means of FLAPW band calculations carried out for four different electronic structures of Ce. The calculated results support the picture of a 4f localized-itinerant transition at the  $\gamma$ - $\alpha$  transition.

Проведено изучение  $\gamma$ - $\alpha$  изоструктурного перехода в Ce посредством зонных расчетов 4f различных электронных структур Ce (методом ЛППВ с потенциалом общего вида). Результаты вычислений приводят к выводу о том, что это переход типа локализация-делокализация для 4f электронной подсистемы церия.

### **1. Introduction**

From numerous experimental data it is known that the  $\gamma$ -phase of metallic cerium is magnetic, having a magnetic moment consistent with a single occupied 4f<sub>5/2</sub> atomic level,  $\alpha$ -cerium is a paramagnetic metal [1].

Besides, it is possible to subdivide cerium compounds into two large groups. The main criterion is the presence or absence of localized magnetic moments at cerium centres. Moreover, it was found that this difference can be observed in the inverse photoemission spectra. The  $\alpha$ -type spectra contain a large peak just above the Fermi level, and the  $\gamma$ -type spectra do not contain such a peak [2].

Up to now, although the cerium problem has a rich prehistory, there are different viewpoints on the nature of the  $\gamma$ - $\alpha$  phase transition. The first "promotional model" puts the energy of a single occupied f-level below the Fermi level for the  $\gamma$ -phase and just above the Fermi level for the  $\alpha$ -phase. Hence, the number of f-electrons on the cerium centre  $n_f$  is nearly unity for the  $\gamma$ -phase and zero for the  $\alpha$ -phase. But this important consequence of the promotional theory is not supported by the so-called high energy experiments (see positron annihilation data [3], Compton profile data [4, 5], muon spin rotation data [6]). Moreover, these experiments indicate that the number of f-electrons is similar for both phases. The alternative approach assumes the description of the isostructural  $\gamma$ - $\alpha$  phase transition as a Mott-type transition [7]. In our opinion this description is the most realistic one. In this case the cerium 4f electron density with two spin components is transferred to the 4f atomic density of  $\gamma$ -cerium. The localized 4f electrons are characterized then by definite (but unknown previously) spin directions. Hence, this is a spin symmetry breaking transition, but in both phases  $n_f$  is nearly unity which is in accordance with experimental data.

<sup>1)</sup> Leninskii Prospekt 31, SU-117915 Moscow, USSR.

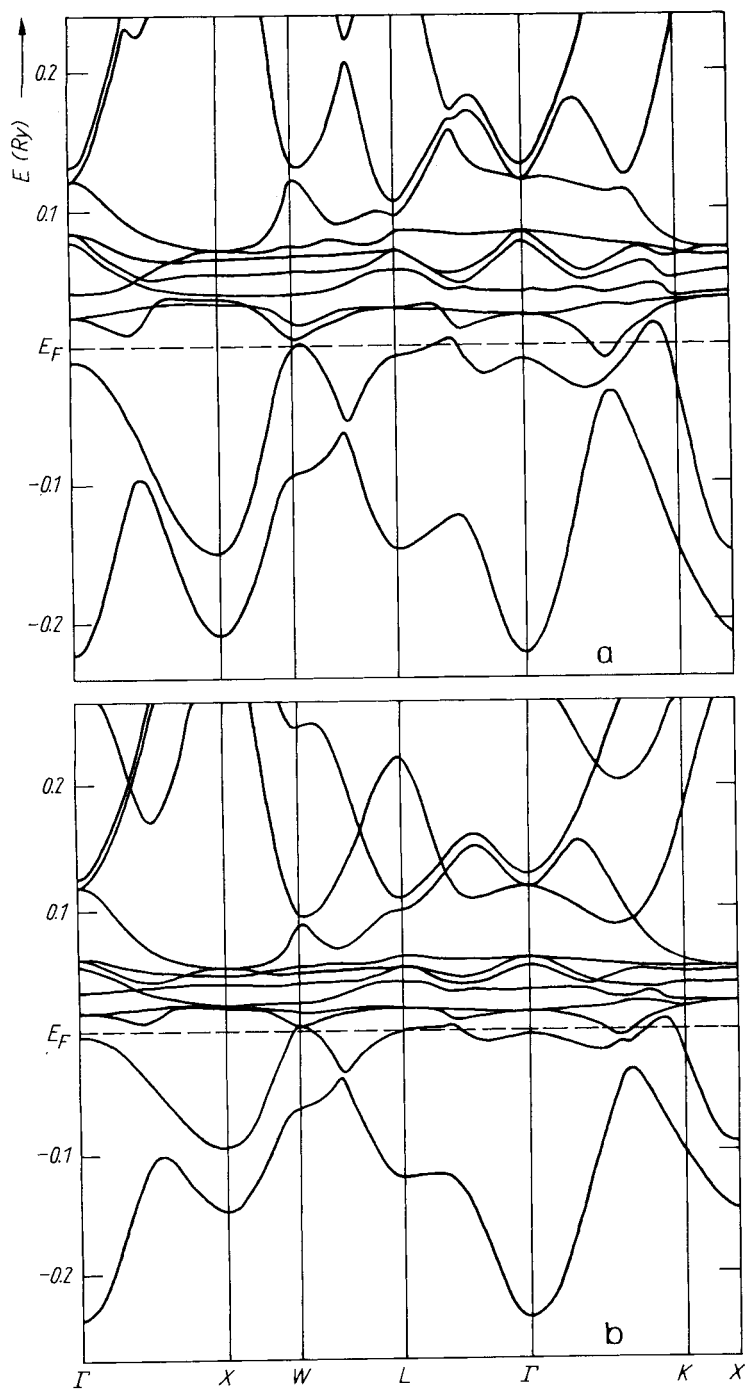


Fig. 1. The band structure for (4)-Ce. a)  $\alpha$ -phase, b)  $\gamma$ -phase

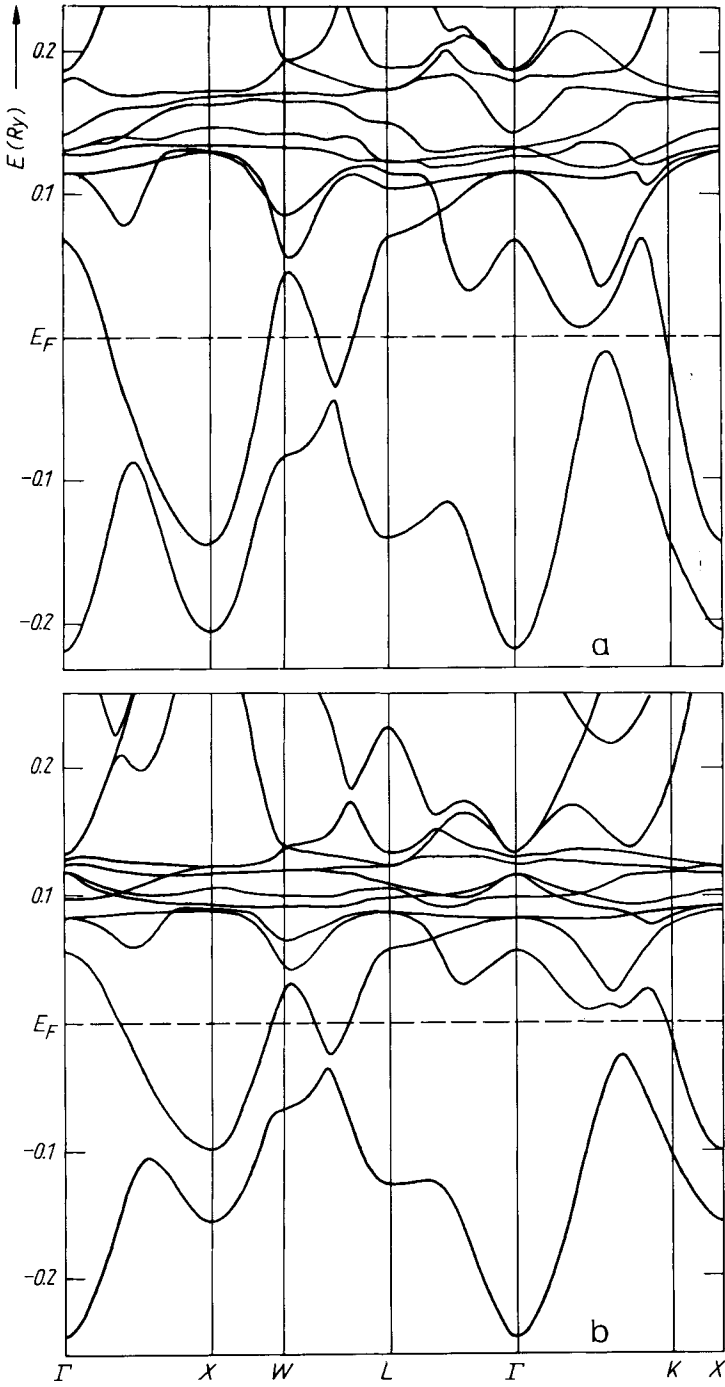


Fig. 2. The band structure for  $(3 + 1)$ -Ce. a)  $\alpha$ -phase, b)  $\gamma$ -phase

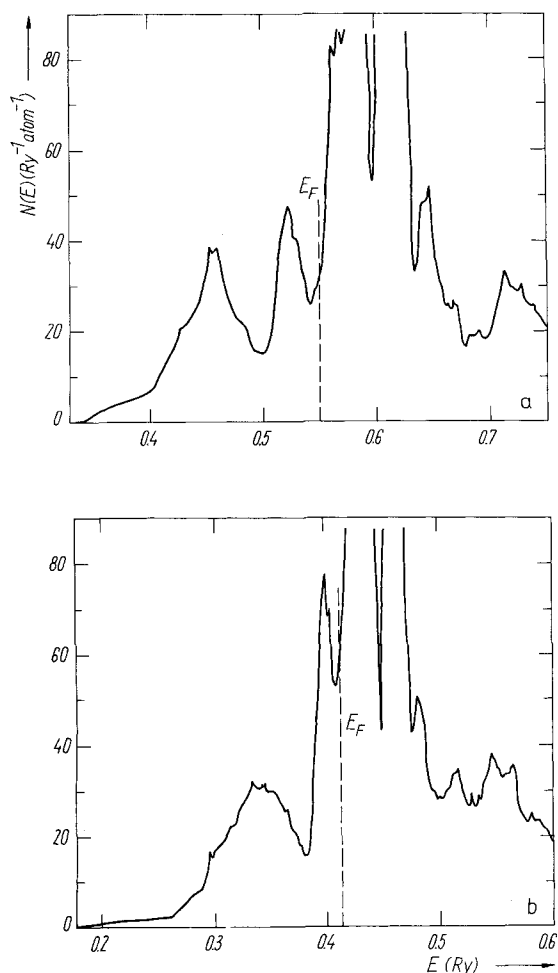


Fig. 3. The density of states of (4)-Ce.  
a)  $\alpha$ -phase, b)  $\gamma$ -phase

In the actinides the consideration of 5f bonding is important with respect to the transition from itinerant to localized states across this series. For the more localized 4f states, the corresponding transition may occur entirely at the  $\gamma$ - $\alpha$  transition in Ce [8].

The idea of the Mott-type transition was firstly suggested in experimental works [9]. It was developed by Johansson [10, 11] and others [8 to 14].

In this paper we offer the band description of the Mott-type transition in cerium.

## 2. Calculation Procedure

We used the LAPW (linear-augmented-plane-wave) method with the full potential proposed and developed by Koelling and Arbman [15]. This method is based on the density functional theory (DFT) with the local density approximation (LDA). (We used the Barth-Hedin approximation [16].)

This method allows to define the probability that the electrons inside a muffin-tin sphere are of s-, p-, d-, f-type and to introduce the corresponding projection operators [15]. We

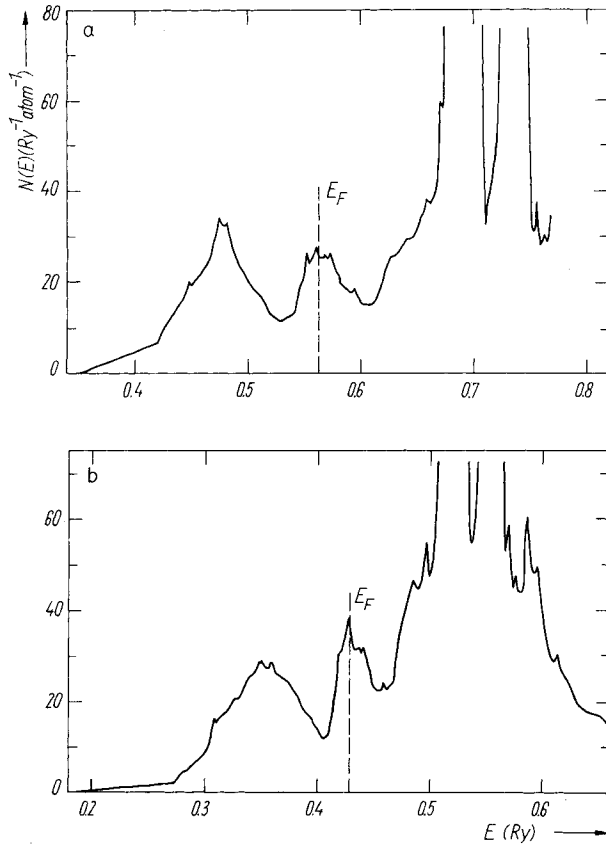


Fig. 4. The density of states of (3 + 1)-Ce. a)  $\alpha$ -phase, b)  $\gamma$ -phase

shall use the occupation numbers  $n_s$ ,  $n_p$ ,  $n_d$ ,  $n_f$  or the partial charges (normalized by the valence electron number).

50 to 60 basis functions are used in the secular equations. Core states were not held frozen but were obtained in each iteration in a single-site approximation. The final convergence in the self-consistent process was  $10^{-5}$  Ryd for the 20-points set of the IBZ. The lattice constants were taken from [13], but the MT sphere radii were chosen as large as possible,  $R_1 = 3.2014$  at.units and  $R_2 = 3.4483$  at.units for  $\alpha$ - and  $\gamma$ -cerium. The plots of band structure (Fig. 1 and 2) were obtained from band calculations with spin-orbit (SO) interaction using 150 first-principles points. Density of states (DOS) curves were obtained by using linear interpolation scheme over 864 tetrahedra of the IBZ (with SO interaction, too, Fig. 3 and 4).

Unlike in other calculations we have done cerium FLAPW calculations with localized f-electrons and evaluated Mott criteria for the cerium f-subsystem.

### 3. The Weak-Coupling Model

The application of the weak-coupling model requires to perform a band structure calculation in which the single 4f orbital is treated like an incompletely occupied core state with a fixed occupation number equal to one [14]. The metallic band in this case is formed from the residual three electrons per cerium centre. We shall mark this type of calculation by the

symbol (3 + 1). The symbol (4) marks the standard band structure calculations with four electrons per cerium centre forming the metallic band.

We have made four types of cerium calculations:  $\alpha$ -phase in (4) and (3 + 1) structures and  $\gamma$ -phase in (4) and (3 + 1) structures.

#### 4. Review of Cerium Band Structures

The main calculation results are shown in Fig. 1 to 4 and Tables 1 and 2. One can see that the cerium band structure is quite different from that with nearly free electrons. The middle of the f-bands (flat parts of the bands) giving rise to a huge peak of the DOS curve (Fig. 3 and 4) is just above the Fermi level for (4)-cerium. The middle of the f-bands of (3 + 1)-cerium is significantly higher than the Fermi level and the f-contribution to the electron states at the Fermi level is small enough due to the rapid decrease of the f-contribution at energy lowering.

The characteristic feature of DOS curves (Fig. 3 and 4) is the two-peak shape corresponding to the photoemission spectral (PES) data (although there are contradictory opinions on the nature of these peaks [17] (see Section 7)). It is interesting that in going from (3 + 1)-cerium to (4)-cerium and from  $\gamma$ -Ce to  $\alpha$ -Ce the band width is almost unchanged (Table 2). Another very important result is the constancy of the f-occupation number in the  $\alpha$ - and  $\gamma$ -phases of (4)-Ce. This value is close to unity (Table 1). Hence, it is probable that the cerium f-electron subsystem undergoes a Mott-type transition.

#### 5. Estimation of the Mott Criteria

Here we shall evaluate the Mott criteria for cerium. Analysing metal-insulator transitions, Mott suggested two quantitative criteria — a geometric one and an energetic one. Mott used the model in which the metallic centre has one valence electron [7]. The cerium metallic

Table 1

Decomposed charge density of Ce;  $A$  lattice constant (in at.units),  $n_s$  to  $n_f$  partial charges (number of electrons per centre)

Ce	$A$	$n_s$	$n_p$	$n_d$	$n_f$	out of MTS
(3 + 1)- $\gamma$	9.7533	0.425	0.166	1.485	1 + 0.184	0.821
(4)- $\gamma$	9.7533	0.422	0.166	1.558	1.071	0.851
(4)- $\alpha$	9.0550	0.314	0.132	1.670	1.074	0.930
(3 + 1)- $\alpha$	9.0550	0.328	0.128	1.555	1 + 0.233	0.896

Table 2

Band structure results for cerium,  $B$  band width (in Ryd),  $U^*$  (f-f) effective f-f repulsion energy (in Ryd),  $Q$  effective charge or valency of Ce,  $N(E_F)$  DOS at the Fermi level (in Ryd<sup>-1</sup> atom<sup>-1</sup>),  $\lambda$  mass enhancement,  $E_{bot}$  bottom of the band (in Ryd)

Ce	$E_{bot}$	$E_F$	$B$	$U^*(f-f)$	$Q$	$N(E_F)$	$\lambda$
(3 + 1)- $\gamma$	0.185	0.430	0.245	0.374	3.16	35.9	0.21
(4)- $\gamma$	0.174	0.413	0.239	0.764	3.28	64.3	-0.33
(4)- $\alpha$	0.327	0.551	0.224	0.652	3.58	32.0	0.90
(3 + 1)- $\alpha$	0.343	0.562	0.219	0.313	3.45	26.9	1.26

centre has in fact four tightly interacting valence electrons. However, due to its great Coulomb repulsion energy the f-electron has a trend to localize (see Appendix). So we use the Mott criteria for the analysis of this trend in application to the cerium f-electron.

1. Geometric criterion [7]:  $M_1 = n^{1/3} R_f = (4n_f)^{1/3} R_f / A$ . Here  $n$  is the averaged f-electron density,  $R_f$  the averaged f-electron radius,  $n_f$  the number of f-electrons (per centre),  $A$  the lattice constant. For  $\gamma$ -Ce we have  $R_f = 1.098$  at.units and  $M_1 = 0.183$ , for  $\alpha$ -Ce  $R_f = 1.097$  and  $M_1 = 0.197$ . This range of values is close to the Mott one for the transition range:  $M_1 \approx 0.18$  to  $0.20$  [7].

2. Mott used also the energetic criterion  $M_2 = W/B$  [7]. There is a competition between energy gain from electron movement (which is evaluated from the band width  $B$ ) and Coulomb repulsion of electrons with different spin orientations (which evaluated from  $W$ ). Here  $W = U^*(f-f) (n_f/2)^2$ ,  $U^*(f-f)$  is the effective Hubbard parameter for f-electrons (see Appendix) which is shown in Table 2. As a result for  $\alpha$ -Ce we have  $W = 0.188$  Ryd,  $B = 0.224$  Ryd, and  $M_2 = 0.839$  and for  $\gamma$ -Ce  $W = 0.219$  Ryd,  $B = 0.239$  Ryd, and  $M_2 = 0.916$ . One obtains that  $M_2 \approx 1$  in accordance with the Mott prediction for such type of transition.

Now we shall discuss the density of states at the Fermi level.  $N(E_F)$  will denote the value for both spins. If we take the linear specific heat coefficient  $\gamma$  from experiments and  $N(E_F)$  from the band structure calculations, the relation

$$\gamma = \frac{\pi^2}{3} k_B^2 (1 + \lambda) N(E_F) \quad (1)$$

gives us the specific-heat mass enhancement  $\lambda$ . This value is determined mostly by electron-photon interaction and is convenient for comparison between theory and experiment. We used  $7.5$  mJ/(mol K<sup>2</sup>) for  $\gamma$ -Ce and  $10.5$  mJ/(mol K<sup>2</sup>) for  $\gamma$ -Ce [13]. One can clearly see that hypothetical structures as  $(3 + 1)$ - $\alpha$ -Ce and  $(4)$ - $\gamma$ -Ce correspond to unrealistic values  $\lambda$  in Table 2 (for the  $\gamma$ -phase  $\lambda < 0$  and for the  $\alpha$ -phase  $\lambda > 1$ ). These are further reasons for supporting a Mott-type transition of the f-electron subsystem.

## 6. Consideration of Cerium with Localized f-Electrons

The low density side of the usual Mott transition corresponds to cerium metal with separately localized f-electrons which weakly interact with the conduction electrons. Here we concern the question of elementary excitations. Although one has no strong formal underpinning for the application of a DFT-like approach to excited states, one can argue that it is not an unreasonable beginning. Moreover, two things this approach deals with in a reasonable fashion are the variations in the kinetic energy and the direct Coulomb energy. These are the major energy terms that are used in the Anderson and Hubbard Hamiltonians [18].

Table 3  
The energy of localized single-particle 4f electronic states (in Ryd)

Ce	$\varepsilon_f - E_F$	$\varepsilon_f^* - E_F$	$\langle \varepsilon_f \rangle - E_F$
$(3 + 1)$ - $\gamma$	0.074	-1.176	-0.551
$(3 + 1)$ - $\alpha$	0.097	-1.127	-0.514

As for cerium, we found that the energy of the localized f-electrons is above the Fermi level for both phases (see  $\varepsilon_f$  in Table 3). So one would expect that, to achieve a minimum of the total energy, the f-electron should go from a localized to an itinerant state. But in fact this transition leads to the low-lying energy level of an unoccupied orbital at the cerium centre ( $\varepsilon_f^*$  in Table 3). This contradiction is closely related with the fact that the energy of the localized f-electron does not coincide with the ionization energy needed to remove this f-electron (like in Coopman's theorem), but is the derivative of the total energy with respect to the occupation number [19],

$$\varepsilon_f = \frac{\partial E}{\partial n_f}. \quad (2)$$

On the other hand, it is well known that the DFT–LDA theory is correct for closed shells only. This is not true in our case. In the calculation procedure the localized f-electron density is divided into two equal parts corresponding to spin-up and spin-down directions, so we automatically “turn on” Coulomb interaction between them. A part of this artificially introduced interaction is compensated by the exchange contribution, but this compensation, due to the use of the LD approximation, is not complete. Hence, one can see that the localized f-electron energy increases [19].

Slater proposed the use of (2) for determining the ionization energy, but unfortunately this relation does not work in our case. Removing the localized f-electron leads to the appearance of the f-hole which strongly interacts with the conduction electrons. Appearance of this f-hole breaks the translation symmetry of a crystal and makes it impossible to estimate the ionization energy by usual band structure calculations. We can only write the following relation [18]:

$$I_f = \frac{\varepsilon_f + \varepsilon_f^*}{2} + \varepsilon_0 = \langle \varepsilon_f \rangle + \varepsilon_0. \quad (3)$$

If the valence density remains constant, then  $-\langle \varepsilon_f \rangle$  is the ionization energy,  $\varepsilon_0$  the relaxation energy of valence density. Comparison between  $\varepsilon_f$  and  $\langle \varepsilon_f \rangle$  in relation to the Fermi level (Table 3) clearly shows that  $\gamma$ -cerium has lower energy of the localized f-electron.

Hence, one would expect that the f-orbital described by (3) is below the Fermi level for the  $\gamma$ -phase and is above the Fermi level for the  $\alpha$ -phase. This would mean that the structure of  $(3 + 1)\text{-}\gamma\text{-Ce}$  is stable and the structure of  $(3 + 1)\text{-}\alpha\text{-Ce}$  is unstable. Supposing that the value  $\varepsilon_0$  in (3) is approximately the same for both phases of cerium, one can obtain the estimation for the energy of the localized f-electron for  $\gamma$ -cerium

$$-0.037 \text{ Ryd } (0.5 \text{ eV}) < I_f - E_F < 0. \quad (4)$$

Hence, in this energetic range the two different types of solution — localized and itinerant — coexist.

## 7. Interpretation of Cerium PE Data

Thanks to the advance in PE and IPE techniques we have at our disposal the high resolution cerium spectra [17, 20 to 23]. PE data show two peaks both for  $\gamma$ - and  $\alpha$ -phases. Supposing that the PE spectral intensity is proportional to the DOS plot of the filled band (as it usually is) one can see that band structure calculations indeed reflect this important spectral property (see Fig. 3 and 4).



However, from band structure calculation we know that the peak near the Fermi energy has pure f-character, and the second deeper peak has (s-d)-character, due to the (s-d)-contribution. This is an important contradiction with experiments which show that both peaks have f-character [17].

The calculated energy distance between these two peaks also differs from the experimental one: band calculations give 1.0 to 1.3 eV, while from spectral data it follows that the energy is approximately 2 eV [21]. At the same time it is possible to show by spectral subtraction that the f-peak of  $\alpha$ -cerium is sharp at the Fermi energy and the f-peak of  $\gamma$ -cerium is soft [22]. We suppose that this is an experimental basis to interpret the f-peak of  $\alpha$ -cerium as being dependent on the contribution of the itinerant f-states.

IPE spectra of  $\alpha$ -cerium exhibit a sharp peak just above the Fermi energy [23]. Band calculations (see Fig. 3) reproduce this peak for  $\alpha$ -cerium and move it to higher energy for  $\gamma$ -cerium. There is some progress, but at the same time IPE spectra of  $\gamma$ -cerium do not contain a sharp peak at high energy [23].

### 8. Conclusion

There is some difference between an ordinary Mott transition and the  $\gamma$ - $\alpha$  phase transition in cerium. The main difference is that both  $\gamma$ - and  $\alpha$ -cerium are metals. Hence, we can interpret  $\gamma$ -cerium as a metal with magnetic impurity in each centre, i.e. a localized f-electron with moment  $J = 5/2$ . Such systems are called dense Kondo lattice and they exhibit abnormal properties.  $\alpha$ -cerium is a correlated metal with large  $\lambda$ .

### Appendix

In the LAPW method we used the density decomposition (s-, p-, d-, and f-). Extracting partial densities one can estimate Coulomb interaction energy (electrostatic in nature) induced by the above-mentioned decomposition,

$$U(l_1-l_2) = \frac{\int \varrho_1(x_1) |x_1 - x_2|^{-1} \varrho_2(x_2) dx_1 dx_2}{\int \varrho_1(x_1) dx_1 \int \varrho_2(x_2) dx_2} \quad (6)$$

These are the values that are shown in Table 4 for (4)- $\gamma$  and (4)- $\alpha$  cerium.

Table 4  
The Coulomb integrals  $U(l_1-l_2)$  of (4)-Ce (in Ryd)

$\alpha \backslash \gamma$	s	p	d	f
s	0.670	0.703	0.689	0.805
p	0.732	0.762	0.727	0.950
d	0.792	0.922	0.723	0.844
f	0.742	0.806	0.766	1.487
	0.875	1.077	0.877	1.418

Unlike in Mott and Hubbard models with one electron per centre, the cerium centre has four valence electrons with strong interaction between them. Our data for the ground state configuration  $f^1d^1s^2$  are:

$$\begin{aligned} U(s-s) &= 0.429 \text{ Ryd}, & U(d-d) &= 0.661 \text{ Ryd}, & U(f-f) &= 1.805 \text{ Ryd}, \\ U(s-d) &= 0.496 \text{ Ryd}, & U(s-f) &= 0.558 \text{ Ryd}, & U(d-f) &= 0.855 \text{ Ryd}. \end{aligned}$$

When forming metallic bonding these parameters, except  $U(f-f)$ , become approximately equal to each other. A correct description of this system is possible only in the framework of the so-called extended Hubbard model taking into account nondiagonal Coulomb parameters (Table 4). While the values of these parameters are sufficiently large, the ground state of the system is metallic. To use the Mott analysis of the system we have to introduce an effective Coulomb repulsion parameter for f-electrons.

We see that all Coulomb parameters except  $U(f-f)$  are nearly equal to  $U(d-d)$ . Besides, a great part of the valence electron density is the d-type density (Table 2). Hence, we can introduce the effective Hubbard energy  $U^*(f-f) = U(f-f) - U(d-d)$ . Now this notion characterizes the trend for localization of cerium f-electrons and leads to different values for  $\gamma$ - and  $\alpha$ -phase.

## References

- [1] D. C. KOSKENMAKI and E. A. GSCHNEIDNER, JR., Handbook on the Physics and Chemistry of Rare Earths, Vol. 1, North-Holland Publ. Co., Amsterdam 1978 (p. 337).
- [2] F. U. HILLEBRECHT and M. CAMPAGNA, Handbook on the Physics and Chemistry of Rare Earths, Vol. 10, North-Holland Publ. Co., Amsterdam 1987 (p. 425).
- [3] R. F. GEMPEL, D. R. GUSTAFSON, and J. D. WILLENBERG, Phys. Rev. B **5**, 2082 (1972).
- [4] J. FELSTEINER, M. HEILPER, and K.-F. BERGGREN, Solid State Commun. **32**, 343 (1979).
- [5] U. KORNSTADT, R. LASSER, and B. LENGELER, Phys. Rev. B **21**, 1898 (1980).
- [6] H. WEHR, K. KNORR, F. N. GYGAX, A. SCHENCK, and W. STUDER, Phys. Rev. B **24**, 4041 (1981).
- [7] N. F. MOTT, Metal-Insulator Transitions, Taylor & Francis, London 1974.
- [8] H. L. SKRIVER, O. K. ANDERSEN, and B. JOHANSSON, Phys. Rev. Letters **41**, 42 (1978).
- [9] D. R. GUSTAFSON, J. D. MCNUTT, and L. O. ROELLIG, Phys. Rev. **183**, 435 (1969).
- [10] B. JOHANSSON, Phil. Mag. **30**, 469 (1974).
- [11] B. JOHANSSON, J. Phys. F **7**, 877 (1977).
- [12] O. ERIKSSON, B. JOHANSSON, and M. S. S. BROOKS, Phys. Rev. Letters, in the press.
- [13] W. E. PICKETT, A. J. FREEMAN, and D. D. KOELLING, Phys. Rev. B **23**, 1266 (1981).
- [14] B. I. MIN, H. J. F. JANSSEN, T. OGUCHI, and A. J. FREEMAN, Phys. Rev. B **34**, 369 (1986).
- [15] D. D. KOELLING and G. O. ARBMAN, J. Phys. F **5**, 2041 (1975).
- [16] V. VON BARTH and L. HEDIN, J. Phys. C **5**, 1629 (1972).
- [17] N. MARTENSSON, B. REIHL, and R. D. PARKS, Solid State Commun. **41**, 573 (1982).
- [18] D. D. KOELLING, Internat. J. Quantum Chem. Quantum Chem. Symp. **20**, 377 (1986).
- [19] J. C. SLATER, The Self-Consistent Field for Molecules and Solids, McGraw-Hill Publ. Co., New York 1974.
- [20] D. M. WIELICZKA, J. H. WEAVER, D. W. LYNCH, and C. G. OLSON, Phys. Rev. B **26**, 7056 (1982).
- [21] D. WIELICZKA, M., C. G. OLSON, and D. W. LYNCH, Phys. Rev. B **29**, 3028 (1984).
- [22] F. PATTHEY, B. DELLEY, W.-D. SCHNEIDER, and Y. BAER, Phys. Rev. Letters **55**, 1518 (1985).
- [23] E. WULLLOUD, H. R. MOSER, W.-D. SCHNEIDER, and Y. BAER, Phys. Rev. B **28**, 7354 (1983).

(Received January 24, 1990; in revised form May 25, 1990)